







# Radio Power from a Direct-collapse Black Hole in CR7

Daniel J. Whalen<sup>1,2</sup> , Mar Mezcuca<sup>3</sup> , Avery Meiksin<sup>4</sup>, Tilman Hartwig<sup>5,6,7</sup> , and Muhammad A. Latif<sup>8</sup> 

<sup>1</sup>Institute of Cosmology and Gravitation, University of Portsmouth, Portsmouth PO1 3FX, UK; [daniel.whalen@port.ac.uk](mailto:daniel.whalen@port.ac.uk)

<sup>2</sup>Ida Pfeiffer Professor, University of Vienna, Department of Astrophysics, Tuerkenschanzstrasse 17, A-1180 Vienna, Austria

<sup>3</sup>Institut d'Estudis Espacials de Catalunya (IEEC), Carrer Gran Capità, E-08034 Barcelona, Spain

<sup>4</sup>Institute for Astronomy, University of Edinburgh, Blackford Hill, Edinburgh EH9 3HJ, UK

<sup>5</sup>Kavli IPMU (WPI), UTIAS, The University of Tokyo, Kashiwa, Chiba 277-8583, Japan

<sup>6</sup>Department of Physics, School of Science, University of Tokyo, Bunkyo, Tokyo 113-0033, Japan

<sup>7</sup>Institute for Physics of Intelligence, School of Science, The University of Tokyo, Bunkyo, Tokyo 113-0033, Japan

<sup>8</sup>Physics Department, College of Science, United Arab Emirates University, P.O. Box 15551, Al-Ain, UAE

Received 2020 April 8; revised 2020 May 21; accepted 2020 June 2; published 2020 June 23

## Abstract

The leading contenders for the seeds of the first quasars are direct-collapse black holes (DCBHs) formed during catastrophic baryon collapse in atomically cooled halos at  $z \sim 20$ . The discovery of the Ly $\alpha$  emitter CR7 at  $z = 6.6$  was initially held to be the first detection of a DCBH, although this interpretation has since been challenged on the grounds of Spitzer IRAC and Very Large Telescope X-Shooter data. Here we determine if radio flux from a DCBH in CR7 could be detected and discriminated from competing sources of radio emission in the halo such as young supernovae and H II regions. We find that a DCBH would emit a flux of 10–200 nJy at 1.0 GHz, far greater than the sub-nJy signal expected for young supernovae but on par with continuum emission from star-forming regions. However, radio emission from a DCBH in CR7 could be distinguished from free-free emission from H II regions by its spectral evolution with frequency and could be detected by the Square Kilometre Array in the coming decade.

*Unified Astronomy Thesaurus concepts:* [Supermassive black holes \(1663\)](#); [Intermediate-mass black holes \(816\)](#); [Primordial galaxies \(1293\)](#); [High-redshift galaxies \(734\)](#); [Population III stars \(1285\)](#); [Quasars \(1319\)](#); [Early universe \(435\)](#); [Reionization \(1383\)](#)

## 1. Introduction

Over 300 quasars have now been discovered at  $z > 6$ , including seven at  $z > 7$  (Mortlock et al. 2011; Bañados et al. 2018; Matsuoka et al. 2019). The seeds of these quasars may be supermassive primordial stars that die as direct-collapse black holes (DCBHs) at  $z \sim 20$ . They form when atomic cooling in a  $10^7$ – $10^8 M_{\odot}$  metal-free halo triggers catastrophic baryon collapse at its center, with infall rates of up to  $1 M_{\odot} \text{ yr}^{-1}$  (e.g., Regan & Haehnelt 2009; Latif et al. 2013). These inflows build up a single star that later collapses to a BH at a mass of  $\sim 10^5 M_{\odot}$  (Hosokawa et al. 2013; Woods et al. 2017; Haemmerlé et al. 2018a, 2018b). DCBHs are the leading candidates for the seeds of the first quasars because they are born in high accretion rates in which they grow more quickly than normal Population III star BHs, which form in much lower densities (e.g., Whalen et al. 2004). Less-massive Population III star BHs are also subject to natal kicks that can eject them from their halos (Whalen & Fryer 2012) and do not encounter enough gas at later times to fuel their rapid growth (Smith et al. 2018; see also Mezcuca 2017; Woods et al. 2019).

The discovery of the strong Ly $\alpha$  emitter CR7 at  $z = 6.6$  (Bowler et al. 2012) was originally held by some to be the first detection of a DCBH (or a Population III galaxy; Sobral et al. 2015) because of the detection of He II 1640 Å emission and the absence of metal lines in the initial observations. Subsequent analyses favored a DCBH because of the difficulties associated with forming  $10^7 M_{\odot}$  of Population III stars at the lower limit of metallicity imposed by observations at the time (Hartwig et al. 2016). But this interpretation has since been challenged on the grounds of [O III] 4959 and 5007 Å emission in Spitzer IRAC data (Bowler et al. 2017), [C II] 158  $\mu\text{m}$  emission found by the Atacama Large

Millimeter/submillimeter Array (ALMA; Matthee et al. 2017), and the reanalysis of Very Large Telescope X-Shooter data (Shibuya et al. 2018), which failed to confirm the presence of He II recombination line emission. In particular, the presence of oxygen and carbon was thought to rule out a DCBH in CR7 because they form in zero-metallicity environments.

However, population synthesis and spectral fitting models predict masses of 5–10 million  $M_{\odot}$  for a BH in CR7, well above those of DCBHs at birth, suggesting if one did form in CR7 it had since grown by up to a factor 100 in mass (Agarwal et al. 2016; Pacucci et al. 2017a). If so, one would expect the existence of metals in CR7 because X-rays from the BH are known to trigger star formation and supernova (SN) explosions in its vicinity. Secondary ionizations from energetic photoelectrons enhance free electron fractions and H<sub>2</sub> formation in the gas, which then cools and forms stars (e.g., Machacek et al. 2003). Metals or dust could also obscure He II recombination line emission from the BH.

Radio observations could reveal the existence of a DCBH in CR7 because it could emit synchrotron radiation that could be detected by the next-generation Very Large Array (ngVLA) or epoch of reionization observatories such as the Low Frequency Array (LOFAR) or the Square Kilometre Array (SKA). Recent studies indicate that the amplification of seed magnetic fields by turbulent dynamos could create tangled magnetic fields even in primordial accretion disks (Schober et al. 2012). These fields can then be ordered and further amplified by the rotation of the disk by the  $\alpha\Omega$  dynamo (Latif & Schleicher 2016) and emit strong radio fluxes upon birth of the BH.

However, young SN remnants in a starburst could masquerade as a DCBH by emitting large synchrotron fluxes at early times, and H II regions due to star formation can also be

sources of GHz emission (Reines et al. 2020). The relative strengths of these three sources will determine if the detection of radio emission from CR7 would reveal the existence of a BH there. We have calculated radio fluxes for a DCBH, SN remnants, and H II regions in CR7. In Section 2 we describe our empirical estimates of DCBH fluxes derived from several fundamental planes (FPs) of BH accretion and calculations of radio fluxes due to young SN remnants and H II regions. We compare these fluxes in Section 3 to determine if the detection of radio emission from CR7 could indicate the presence of a BH there.

## 2. Radio Emission from CR7

We consider radio flux from a DCBH, SNe, and H II regions due to the formation of massive stars.

### 2.1. DCBH

Observations have empirically confirmed a correlation between the mass of a BH,  $M_{\text{BH}}$ , its 2–10 keV nuclear X-ray luminosity,  $L_X$ , and its 5 GHz nuclear luminosity,  $L_R$ , known as the FP of BH accretion (Merloni et al. 2003; see Mezcua et al. 2018 for a brief review). This correlation is supported by theoretical models of accretion and extends over six orders of magnitude in mass, including the intermediate-mass black hole regime (Gültekin et al. 2014). There has been some debate if radio-loud and radio-quiet active galactic nuclei (AGNs) occupy distinct regions in the FP but La Franca et al. (2010) and Bonchi et al. (2013) have found no evidence for a bimodality in the radio luminosity function and that the FP is applicable to all types of AGNs.

To estimate the flux from a DCBH in CR7 in a given radio band in the observer frame we first calculate its 5 GHz luminosity in the rest frame with an FP. This requires  $L_X$ , which we find from the bolometric luminosity of the BH with Equation (21) of Marconi et al. (2004),

$$\log\left(\frac{L_{\text{bol}}}{L_X}\right) = 1.54 + 0.24\mathcal{L} + 0.012\mathcal{L}^2 - 0.0015\mathcal{L}^3, \quad (1)$$

where  $\mathcal{L} = \log L_{\text{bol}} - 12$  and  $L_{\text{bol}}$  is in units of solar luminosity. Agarwal et al. (2016) estimate the mass and luminosity of the BH in CR7 to be  $4.4 \times 10^6 M_\odot$  and  $0.4 L_{\text{Edd}}$ , respectively, where  $L_{\text{Edd}} = 1.26 \times 10^{38} (M/M_\odot) \text{ erg s}^{-1}$ . These values yield  $L_X = 1.22 \times 10^{43} \text{ erg s}^{-1}$ , which is consistent with the upper limit  $L_X \lesssim 10^{44} \text{ erg s}^{-1}$  found by Pacucci et al. (2017b).  $L_R$  can then be obtained from any of a number of FPs of the form

$$\log L_R = \alpha \log L_X + \beta \log M_{\text{BH}} + \gamma, \quad (2)$$

where  $\alpha$ ,  $\beta$ , and  $\gamma$  for FPs from Merloni et al. (2003, hereafter MER03), Körtling et al. (2006, hereafter KOR06), Gültekin et al. (2009, hereafter GUL09), Plotkin et al. (2012, hereafter PLT12), and Bonchi et al. (2013, hereafter BON13) are listed in Table 1. We also include the FP of Equation (19) of Gültekin et al. (2019, hereafter GUL19),

$$R = -0.62 + 0.70 X + 0.74 \mu, \quad (3)$$

where  $R = \log(L_R/10^{38} \text{ erg s}^{-1})$ ,  $X = \log(L_X/10^{40} \text{ erg s}^{-1})$  and  $\mu = \log(M_{\text{BH}}/10^8 M_\odot)$ .

Radio flux from CR7 that is redshifted into a given band in the observer frame in general does not originate from 5 GHz in

**Table 1**  
Fundamental Planes

FP	$\alpha$	$\beta$	$\gamma$
MER03	0.60	0.78	7.33
KOR06	0.71	0.62	3.55
GUL09	0.67	0.78	4.80
PLT12	0.69	0.61	4.19
BON13	0.39	0.68	16.61

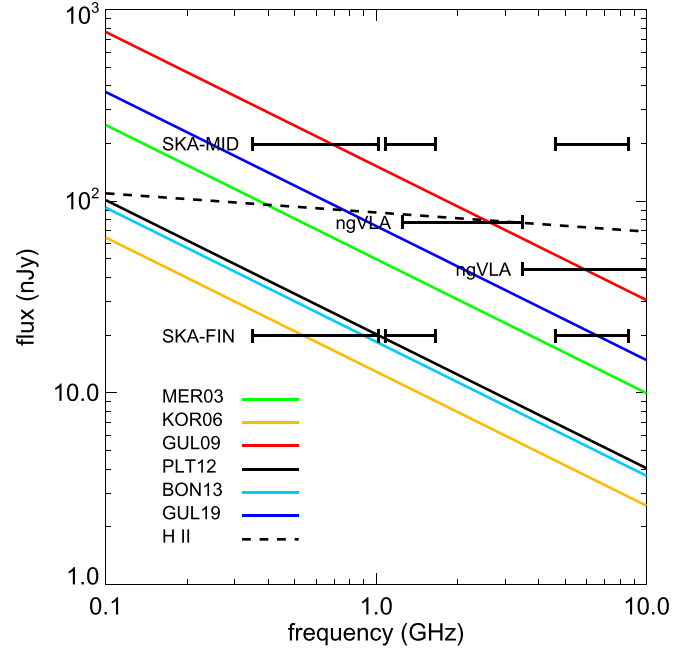


**Figure 1.** CR7 DCBH (solid lines) and H II fluxes (dashed line) predicted by the six FPs from 100 MHz to 10 GHz with detection limits for the SKA-MID and SKA-FINAL surveys and ngVLA sensitivities for 24 hr integration times.

the source frame so we calculate it from  $L_R = \nu L_{\nu'}$ , assuming that the spectral luminosity  $L_{\nu'} \propto \nu'^{-\alpha}$  with a spectral index  $\alpha = 0.7$  (Condon et al. 2002). The spectral flux at  $\nu$  in the observer frame can then be obtained from the spectral luminosity at  $\nu'$  in the rest frame from

$$F_{\nu} = \frac{L_{\nu'}(1+z)}{4\pi d_L^2}, \quad (4)$$

where  $d_L$  is the luminosity distance and  $\nu' = (1+z)\nu$ . If we use second-year Planck cosmological parameters ( $\Omega_M = 0.308$ ,  $\Omega_\Lambda = 0.691$ ,  $\Omega_b h^2 = 0.0223$ ,  $\sigma_8 = 0.816$ ,  $h = 0.677$ , and  $n = 0.968$ ; Planck Collaboration et al. 2016),  $d_A = 1143.8$  Mpc. We plot DCBH fluxes from 100 MHz to 10 GHz for all six FPs in Figure 1.

### 2.2. SN Radio Flux

We first consider the simplest case of SNe due to a starburst. In a starburst, most of the stars form in about the lifetime of any one of them, and 10–20  $M_\odot$  core-collapse (CC) SNe would produce the most synchrotron emission because energetic pair-instability (PI) SNe explode in much lower-density H II regions that emit far less radio energy when swept up by the remnant (Meiksin & Whalen 2013). Elemental abundances measured in a number of extremely metal-poor stars suggest that many stars in the early universe may have been a few tens of solar masses

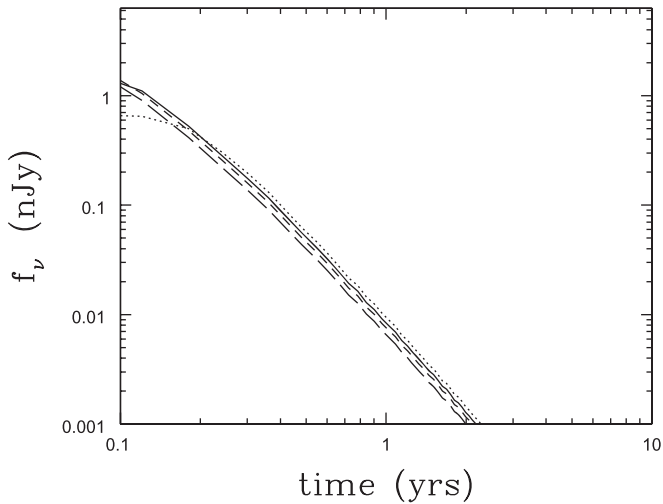


**Figure 2.** Radio synchrotron emission from a  $15 M_{\odot}$  CC SN in a fiducial H II region with an ambient density of  $0.4 \text{ cm}^{-3}$  at  $z = 6.6$ : 0.5 GHz (dotted), 1.4 GHz (solid), 3 GHz (short-dashed) and 8.4 GHz (long-dashed).

(e.g., Joggerst et al. 2010; Ishigaki et al. 2018). The SN rate in a starburst can be obtained by dividing the total mass of Population III stars originally inferred to be in CR7,  $\sim 10^7 M_{\odot}$ , by the average mass of the longest-lived stars capable of producing SNe, which we take to be  $\sim 15 M_{\odot}$ . This yields the maximum number of SNe over the duration of the burst, which would be about the lifetime of a  $15 M_{\odot}$  Population III star,  $\sim 10 \text{ Myr}$ . Dividing the total number of SNe by the duration of the burst yields one Population III SN every 15 yr. Another SN rate can be derived from the Population II star formation rate (SFR) inferred from recent observations of CR7 by ALMA, which is  $\sim 50 M_{\odot} \text{ yr}^{-1}$  (Table 1 of Matthee et al. 2017). Assuming a Salpeter initial mass function with one CC SN per  $60 M_{\odot}$  of stars, this SFR produces about one CC SN per year.

In Figure 2 we show radio fluxes for a single  $15 M_{\odot}$  CC SN at  $z = 6.6$  in densities like those expected for the low-metallicity environments of massive stars in CR7. Ionizing UV flux from the progenitor star first creates an H II region. The star then explodes in ambient densities of  $0.4 \text{ cm}^{-3}$  (halo 2 of Whalen et al. 2008). After the explosion the fluxes peak at  $\sim 0.75\text{--}2 \text{ nJy}$  but then fall by three orders of magnitude in 2 yr (for a detailed description of this calculation, see Meiksin & Whalen 2013). Although the SN peaks above 1 nJy, its average flux over the 15 yr interval between explosions in the Population III starburst would be at least a factor of 10 lower because of its sharp decline in less than a year. We have verified that these fluxes change very little as ambient densities are varied over an order of magnitude, which are typical of H II regions in high-redshift, low-metallicity dwarf galaxies. Even the Population II SFR would yield less than 1 nJy of continuous flux,  $\sim 10\text{--}1000$  times less than that of a DCBH, depending on frequency.

### 2.3. H II Radio Flux

Thermal bremsstrahlung in H II regions can produce continuum radio emission whose spectral radio density can be connected to the ionizing photon rate in the H II region,

$Q_{\text{Lyc}}$ , by

$$L_{\nu} \lesssim \left( \frac{Q_{\text{Lyc}}}{6.3 \times 10^{52}} \right) \left( \frac{T_e}{10^4 \text{ K}} \right)^{0.45} \left( \frac{\nu}{\text{GHz}} \right)^{-0.1} \quad (5)$$

in units of  $10^{20} \text{ W Hz}^{-1}$  (Condon 1992), where  $Q_{\text{Lyc}} = \text{SFR} (M_{\odot} \text{ yr}^{-1}) / 1.0 \times 10^{-53}$  (Kennicutt 1998). We estimate the radio continuum from star-forming regions in CR7 by assuming  $\text{SFR} = 50 M_{\odot} \text{ yr}^{-1}$  and  $T_e = 10^4 \text{ K}$  plot it in Figure 1. It varies from 100 nJy at 100 MHz to 70 nJy at 10 GHz. We take this flux to be an upper limit because it is calibrated for star-forming regions in the local universe today.

### 3. Discussion and Conclusion

Our calculations indicate that radio emission from a DCBH in CR7 could be detected by the SKA and ngVLA. The SKA-MID deep survey will reach sensitivities of 200 nJy in three bands (0.35–1.05, 0.95–1.76, and 4.6–8.5 GHz), while the SKA-FINAL all-sky survey will reach 20 nJy in these bands.<sup>9</sup> The ngVLA could reach 45 nJy at 3.5–12.3 GHz and 78 nJy at 1.2–3.5 GHz in 24 hr integration times (Plotkin & Reines 2018), which would be sufficient to detect the flux in those bands predicted by MER03, GUL09, and GUL19.<sup>10</sup> No surveys for LOFAR would exceed sensitivities of a few  $\mu\text{Jy}$  so it is unlikely to detect any radio emission from CR7. The VLA has already visited the COSMOS legacy fields in which CR7 was originally discovered at 3 GHz with a sensitivity of  $2.3 \mu\text{Jy}/\text{beam}$  (Smolčić et al. 2017) but we found no radio counterpart to CR7 in this archive (none of the FPs predict fluxes of this magnitude).

It is unlikely that radio emission from SNe in CR7 could be mistaken for DCBH emission because their average fluxes would be less than 1 nJy, even from starbursts. This signal would be well below the detection limit of any planned survey and is a factor of 10–100 smaller than even the most pessimistic DCBH fluxes predicted by the FPs. SN radio luminosities compiled for a sample of 19 nearby galaxies (Chomiuk & Wilcots 2009) predict higher average fluxes for the SFRs inferred for CR7 (8.5–85 nJy from 10 GHz to 100 MHz; Section 5.3 of Reines et al. 2020). If these values were true of SN populations in CR7 they could still be distinguished from emission from a DCBH because they are lower than all but two of the fluxes predicted by the FPs. However, it is unlikely that SN remnants in CR7 would emit this much flux. Absorption of ionizing UV by dust in H II regions at solar metallicities today limits them to smaller radii and thus higher densities, and stellar winds also plow up ambient gas and create dense structures in the vicinity of the stars. Ejecta from SNe crashing into these higher densities emit considerably more radio flux than SNe in the diffuse H II regions of low-metallicity environments at high redshift, in which stellar winds are weak if present at all (Whalen et al. 2004).

The continuum radio flux due to H II regions in CR7 could be similar to or even greater than that of a DCBH depending on frequency and choice of FP. However, this flux falls off much more slowly with frequency than DCBH emission so the two could be easily distinguished at frequencies below about 3 GHz by the SKA for half of the FPs. Radio emission due to thermal bremsstrahlung ultimately depends on electron temperatures

<sup>9</sup> [https://www.ectstar.eu/sites/www.ectstar.eu/files/talks/trento\\_Wagg.pdf](https://www.ectstar.eu/sites/www.ectstar.eu/files/talks/trento_Wagg.pdf)





<sup>10</sup> [http://library.nrao.edu/public/memos/ngvla/NGVLA\\_21.pdf](http://library.nrao.edu/public/memos/ngvla/NGVLA_21.pdf)

and densities. Because our estimates here are derived for H II regions in local galaxies, which have higher densities than those in less-massive, high-redshift galaxies, we take them to be a (possibly severe) upper limit to the H II region radio flux from CR7. If the true flux is considerably smaller than ngVLA could still find emission from a DCBH. Otherwise, the detection of a DCBH in CR7 due to disparities in flux from H II regions as a function of frequency may be limited to the SKA.

A unique aspect of high-redshift quasars is that the cosmic microwave background (CMB) can quench radio emission from BH jets. If the energy density of CMB photons exceeds that of the magnetic fields in the lobes of the jet, relativistic electrons preferentially cool by upscattering CMB photons rather than synchrotron radiation, and the lack of radio emission from some high-redshift quasars has been attributed to this process (Fabian et al. 2014; Ghisellini et al. 2014). However, this would not change the fluxes in our calculations because they come from the central region of the quasar, not jets, and jets are not expected at the accretion rates estimated for the BH in CR7 because they have only been observed at  $L \lesssim 0.01 L_{\text{Edd}}$  and  $L \gtrsim L_{\text{Edd}}$ . Finally, we note that while the detection of radio emission could confirm the presence of a BH in CR7, the failure to do so would not rule out its existence. It could be that the radio fluxes associated with DCBH candidates lie below those predicted by FPs today so the discovery of a BH in CR7 may have to await future observatories.

The authors thank the anonymous referee for constructive comments that improved the quality of this Letter, and Bhaskar Agarwal, Philip Best, Simon Glover, and Marta Volonteri for helpful discussions. D.J.W. was supported by UK STFC New Applicant Grant ST/P000509/1 and the Ida Pfeiffer Professorship at the Institute of Astrophysics at the University of Vienna. M.M. acknowledges support from the Beatriu de Pinos fellowship (2017-BP-00114). A.M. acknowledges support from the UK Science and Technology Facilities Council Consolidated Grant ST/R000972/1. T.H. was supported by JSPS KAKENHI grant No. 17F17320. M.L. acknowledges funding from UAEU via UPAR grant No. 31S372.

### ORCID iDs

Daniel J. Whalen  <https://orcid.org/0000-0001-6646-2337>  
 Mar Mezcua  <https://orcid.org/0000-0003-4440-259X>  
 Tilman Hartwig  <https://orcid.org/0000-0001-6742-8843>  
 Muhammad A. Latif  <https://orcid.org/0000-0003-2480-0988>

### References

Agarwal, B., Johnson, J. L., Zackrisson, E., et al. 2016, *MNRAS*, 460, 4003

- Bañados, E., Venemans, B. P., Mazzucchelli, C., et al. 2018, *Natur*, 553, 473  
 Bonchi, A., La Franca, F., Melini, G., Bongiorno, A., & Fiore, F. 2013, *MNRAS*, 429, 1970  
 Bowler, R. A. A., Dunlop, J. S., McLure, R. J., et al. 2012, *MNRAS*, 426, 2772  
 Bowler, R. A. A., McLure, R. J., Dunlop, J. S., et al. 2017, *MNRAS*, 469, 448  
 Chomiuk, L., & Wilcots, E. M. 2009, *ApJ*, 703, 370  
 Condon, J. J. 1992, *ARA&A*, 30, 575  
 Condon, J. J., Cotton, W. D., & Broderick, J. J. 2002, *AJ*, 124, 675  
 Fabian, A. C., Walker, S. A., Celotti, A., et al. 2014, *MNRAS*, 442, L81  
 Ghisellini, G., Celotti, A., Tavecchio, F., Haardt, F., & Sbarrato, T. 2014, *MNRAS*, 438, 2694  
 Gültekin, K., Cackett, E. M., King, A. L., Miller, J. M., & Pinkney, J. 2014, *ApJL*, 788, L22  
 Gültekin, K., Cackett, E. M., Miller, J. M., et al. 2009, *ApJ*, 706, 404  
 Gültekin, K., King, A. L., Cackett, E. M., et al. 2019, *ApJ*, 871, 80  
 Haemmerlé, L., Woods, T. E., Klessen, R. S., Heger, A., & Whalen, D. J. 2018a, *ApJL*, 853, L3  
 Haemmerlé, L., Woods, T. E., Klessen, R. S., Heger, A., & Whalen, D. J. 2018b, *MNRAS*, 474, 2757  
 Hartwig, T., Latif, M. A., Magg, M., et al. 2016, *MNRAS*, 462, 2184  
 Hosokawa, T., Yorke, H. W., Inayoshi, K., Omukai, K., & Yoshida, N. 2013, *ApJ*, 778, 178  
 Ishigaki, M. N., Tominaga, N., Kobayashi, C., & Nomoto, K. 2018, *ApJ*, 857, 46  
 Jogerst, C. C., Almgren, A., Bell, J., et al. 2010, *ApJ*, 709, 11  
 Kennicutt, R. C. J. 1998, *ARA&A*, 36, 189  
 Körtling, E., Falcke, H., & Corbel, S. 2006, *A&A*, 456, 439  
 La Franca, F., Melini, G., & Fiore, F. 2010, *ApJ*, 718, 368  
 Latif, M. A., & Schleicher, D. R. G. 2016, *A&A*, 585, A151  
 Latif, M. A., Schleicher, D. R. G., Schmidt, W., & Niemeyer, J. 2013, *MNRAS*, 430, 588  
 Machacek, M. E., Bryan, G. L., & Abel, T. 2003, *MNRAS*, 338, 273  
 Marconi, A., Risaliti, G., Gilli, R., et al. 2004, *MNRAS*, 351, 169  
 Matsuoka, Y., Onoue, M., Kashikawa, N., et al. 2019, *ApJL*, 872, L2  
 Matthee, J., Sobral, D., Boone, F., et al. 2017, *ApJ*, 851, 145  
 Meiksin, A., & Whalen, D. J. 2013, *MNRAS*, 430, 2854  
 Merloni, A., Heinz, S., & di Matteo, T. 2003, *MNRAS*, 345, 1057  
 Mezcua, M. 2017, *IJMPD*, 26, 1730021  
 Mezcua, M., Hlavacek-Larrondo, J., Lucey, J. R., et al. 2018, *MNRAS*, 474, 1342  
 Mortlock, D. J., Warren, S. J., Venemans, B. P., et al. 2011, *Natur*, 474, 616  
 Pacucci, F., Natarajan, P., & Ferrara, A. 2017a, *ApJL*, 835, L36  
 Pacucci, F., Pallottini, A., Ferrara, A., & Gallerani, S. 2017b, *MNRAS*, 468, L77  
 Planck Collaboration et al. 2016, *A&A*, 594, A13  
 Plotkin, R. M., Markoff, S., Kelly, B. C., Körtling, E., & Anderson, S. F. 2012, *MNRAS*, 419, 267  
 Plotkin, R. M., & Reines, A. E. 2018, arXiv:1810.06814  
 Regan, J. A., & Haehnelt, M. G. 2009, *MNRAS*, 396, 343  
 Reines, A. E., Condon, J. J., Darling, J., & Greene, J. E. 2020, *ApJ*, 888, 36  
 Schober, J., Schleicher, D., Federrath, C., et al. 2012, *ApJ*, 754, 99  
 Shibuya, T., Ouchi, M., Harikane, Y., et al. 2018, *PASJ*, 70, S15  
 Smith, B. D., Regan, J. A., Downes, T. P., et al. 2018, *MNRAS*, 480, 3762  
 Smolčić, V., Novak, M., Bondi, M., et al. 2017, *A&A*, 602, A1  
 Sobral, D., Matthee, J., Darvish, B., et al. 2015, *ApJ*, 808, 139  
 Whalen, D., Abel, T., & Norman, M. L. 2004, *ApJ*, 610, 14  
 Whalen, D., van Veelen, B., O'Shea, B. W., & Norman, M. L. 2008, *ApJ*, 682, 49  
 Whalen, D. J., & Fryer, C. L. 2012, *ApJL*, 756, L19  
 Woods, T. E., Agarwal, B., Bromm, V., et al. 2019, *PASA*, 36, e027  
 Woods, T. E., Heger, A., Whalen, D. J., Haemmerlé, L., & Klessen, R. S. 2017, *ApJL*, 842, L6